Available online at www.sciencedirect.com
SCIENCE DIRECT
Journal of the European Ceramic Society 26 (2006) 1131–1139
www.elsevier.com/locate/jeurceramsoc

Influence of lithium oxide as auxiliary flux on the properties of triaxial porcelain bodies

D.U. Tulyaganov, S. Agathopoulos, H.R. Fernandes, J.M.F. Ferreira *

Department of Ceramics and Glass Engineering, University of Aveiro, CICECO, 3810-193 Aveiro, Portugal

Received 21 April 2004; received in revised form 29 January 2005; accepted 30 January 2005
Available online 23 February 2005

Abstract

The influence of Li_2O-content on the properties of standard triaxial porcelains was investigated. Two series of porcelain formulations were produced. The first one comprised seven model formulations with increasing amount of Li_2CO_3 (1–7 wt.%), with respect to the standard triaxial porcelain formulation. The experimental results showed that desirable properties for tableware porcelains can be attained if the Li_2O-content does not exceed ~1.5 wt.%. In the light of this conclusion, the second series of formulations aimed at producing new porcelains using Li-bearing natural rocks. Under an industrial perspective, the most important finding is that these compositions matured at temperatures 100–120 °C lower than the standard triaxial porcelain formulation and exhibited remarkable resistance at over-firing conditions. The role of increasing Li_2O-content at the different stages of firing is interpreted in the light of its influence on densification, the evolution of crystalline phases and microstructure.

Keywords: Li_2O; Firing; Microstructure final; Mechanical properties; Porcelains

1. Introduction

Porcelains, the foundation of ceramic industry, are referred to as triaxial whiteware bodies because of their three-part composition of clay, feldspar and quartz.[1] Traditional hard porcelain bodies are typically mixtures of 50% fine-grained clay, 25% fluxes (usually feldspar) and 25 flint (quartz) (in wt.%), which mature at temperatures between 1350 and 1450 °C.[2] In the frame of global competition, the current trend in whiteware processing is directed towards substantial reduction of capital and running costs without compromising productivity and product quality. To reduce energy consumption, development of advanced energy efficient equipments has mainly attracted the interest. However, an important approach of the overall problem is the lowering of firing temperature and time, which mainly depend on the formulation of the batch of the raw materials.

For instance, small fraction of synthetic zinc or calcium borate in tableware, electrical and sanitaryware porcelain formulations resulted in substantial reduction of firing temperature and broadening of useful firing range.[3] Similar results, i.e. early densification of materials and widening of maturing range, were obtained in the case of incorporation of 5–8 wt.% ZnO-containing glaze in a conventional tableware porcelain formulation.[4]

Lithium aluminosilicates, such as spodumene, have been also used as raw materials in the production of thermal-shock resistant whiteware and sanitaryware.[5,6] The presence of spodumene causes enhancement of mullitization degree and imparts better physical and mechanical properties to ceramics.[7] In general, the Li_2O–Al_2O_3–SiO_2 systems are well known for their low or even negative thermal expansion coefficients. Thus, intensive effort has been directed at producing ceramics which contain β-eucryptite and β-spodumene with relatively high content of Li_2O.[8–10] β-Eucryptite and β-spodumene containing porcelains, with 8.03–11.86 wt.% Li_2O, have been produced using kaolin, quartz and Li_2CO_3 as raw materials via conventional ceramic

* Corresponding author. Tel.: +351 234 370242; fax: +351 234 425300.
E-mail address: jmf@cv.ua.pt (J.M.F. Ferreira).

0955-2219/$ – see front matter © 2005 Elsevier Ltd. All rights reserved.
doi:10.1016/j.jeurceramsoc.2005.01.036

Table 1
Chemical composition of raw materials (wt.%)

Oxides (wt.%)	Kaolin	Ball clay	Silica sand	Feldspar	Rock A[a]	Rock B[a]
SiO_2	47.83	60.96	96.18	66.91	72.76	71.05
Al_2O_3	36.86	23.98	1.25	18.22	16.88	17.74
Fe_2O_3	0.67	0.67	0.16	0.13	0.23	0.18
CaO	0.07	0.84	0.70	0.27	0.10	0.04
MgO	0.30	0.58	–	0.12	0.09	0.02
Na_2O	0.10	0.36	0.13	2.55	1.15	2.58
K_2O	1.65	2.25	1.08	11.75	4.73	3.58
TiO_2	0.02	1.18	–	0.02	0.04	0.04
Li_2O	–	–	–	–	2.36	1.76
P_2O_5	–	–	–	–	0.24	0.71
L.O.I.	12.5	10.67	0.67	–	1.24	1.99

[a] Rock A and rock B: Li-bearing pegmatites A and B, respectively. These Li-rich aplite–pegmatite dykes, kindly offered by the Centre of Geology of the University of Porto, were obtained from a deposit (Covas de Barroso district, northern Portugal), whose Li_2O-content varies between 0.9 and 3.0 wt.%. The results of mineralogical and purification studies of these natural rocks have been published elsewhere (see Table 4).[20,21] These rocks can be generally classified as pegmatites which bear lithium minerals, specifically α-spodumene (rock A) and α-petalite (rock B). They also contain potassium and sodium feldspar, quartz and muscovite.

techniques.[10] Mullite–spodumene composites have been produced from kaolin and Li_2CO_3, incorporated in the batch in the amount of 1–5 wt.%.[11] That work focused on crystalline phase evolution upon firing but there is no information about the role of Li_2O on sintering and maturation of porcelain bodies.

Although triaxial porcelain systems have been long and extensively documented,[12–19] there is no systematic investigation on the influence of lithium oxide, as auxiliary flux, on the processing and the properties of triaxial porcelain bodies. The present work addresses itself to this aim. In particular, we produced model formulations of Li_2O-doped standard triaxial porcelains, whose batches contained 1–7 wt.% Li_2CO_3. The evaluation of the sintering behaviour of these model porcelains allowed us to design and produce new formulations of porcelains for industrial and commercial use, where Li_2O was introduced in the batch via natural lithium-bearing pegmatite. The physical and the mechanical properties, together with the microstructure and the crystalline phase analyses of these porcelains are presented.

2. Materials and experimental procedure

As mentioned in the Introduction, two series of porcelain bodies were investigated. The model formulations were produced using kaolin (Standard Porcelain, ECC International Ltd, UK), quartz sand (P500, Sibelco Portuguesa S.A., Portugal), feldspar (FKI, Felmica, Portugal) and reagent grade Li_2CO_3 (Aldrich, >99%, UK). Table 1 presents the chemical composition (in wt.%) of these raw materials. The composition of standard triaxial porcelain, denoted as L0, was our reference formulation. Seven model formulations, with increasing amounts of Li_2O (with respect to L0), designated from L1 to L7 (the number refers to the wt.% of Li_2CO_3 in the batch), were produced in laboratory conditions via dry-pressing and sintering. Table 2 summarizes the batch formulations and the chemical compositions of the model porcelains (in wt.%).

Homogenous batches of feldspar (mean particles size ~8 μm), quartz sand, kaolin and Li_2CO_3 were prepared by dry-mixing in a porcelain jar. Pellets of 20 mm in diameter and 3–4 mm in height were produced by uniaxially pressing at 80 MPa and firing in laboratory electrical furnace at 1100,

Table 2
Batch formulations and chemical compositions of the model porcelain bodies

	L0	L1	L2	L3	L4	L5	L6	L7
Kaolin	50.00	49.50	49.00	48.50	48.00	47.50	47.00	46.50
Quartz	25	24.75	24.50	24.25	24.00	23.75	23.50	23.25
Feldspar	25	24.75	24.50	24.25	24.00	23.75	23.50	23.25
Li_2CO_3	0.00	1.00	2.00	3.00	4.00	5.00	6.00	7.00
SiO_2	69.10	68.80	68.50	68.20	67.78	67.55	67.24	66.92
Al_2O_3	24.89	24.79	24.67	24.56	24.41	24.34	24.33	24.11
Fe_2O_3	0.44	0.43	0.43	0.42	0.42	0.42	0.42	0.42
CaO	0.30	0.28	0.29	0.29	0.28	0.29	0.28	0.28
MgO	0.18	0.19	0.19	0.20	0.19	0.19	0.19	0.19
Na_2O	0.77	0.76	0.76	0.76	0.76	0.76	0.75	0.74
K_2O	4.32	4.30	4.27	4.25	4.22	4.21	4.19	4.17
TiO_2	0.01	0.01	0.01	0.01	0.01	0.01	0.01	0.01
LiO_2	0.0	0.44	0.88	1.32	1.92	2.23	2.69	3.16

Table 3
Formulations (in wt.%) of the porcelains A and B, containing Li-bearing pegmatite (rock A and rock B, Table 1)

Formulation	Kaolin	Ball clay	Rock A	Rock B	Quartz
A	42	8	35	–	15
B	42	8	–	31	19

1150, 1200, 1250, 1300 and 1350 °C (heating and cooling rates 5°/min and 1 h soaking at the highest temperature). Five samples of each model composition were subjected to each firing test.

The production of the samples of the second series of the investigated formulations employed plastic forming techniques using aqueous media. Two compositions, named as A and B (Table 3), were produced using two different types of Li-bearing pegmatite, named as rock A and rock B (see the note of Tables 1 and 4),[20,21] kaolin, ball clay (ADM, Portugal) and quartz sand. Table 1 presents the chemical composition of rock A, rock B and ball clay. For comparison purposes, samples of standard triaxial porcelain formulation (42% kaolin, 8% ball clay, 25% feldspar, and 25% quartz), named as L (which resembles L0), were produced using the same processing method.

The coarse grains of the as-received lithium rocks were milled in aqueous media, resulting in powders with a mean particle size of about 6–7 μm (Fig. 1). Then, fine quartz sand, kaolin and ball clay were added and mixed together to get a homogeneous slurry (solid/water = 50/50, in wt.%). The tested specimens were obtained by plastic forming technique. The specimens were dried at 50 °C and then at 110 °C. Firing was carried out in laboratory electrical furnace at several temperatures between 1050 and 1300 °C (heating rate 4°/min, soaking time at highest temperature 1 h). Firing was also realized in an industrial tunnel kiln furnace, where the firing temperature ranged between 1365 and 1380 °C (bottom and top positions in the kiln, respectively), the firing circle was ∼25 h, and the soaking time at the firing zone was ∼1 h.

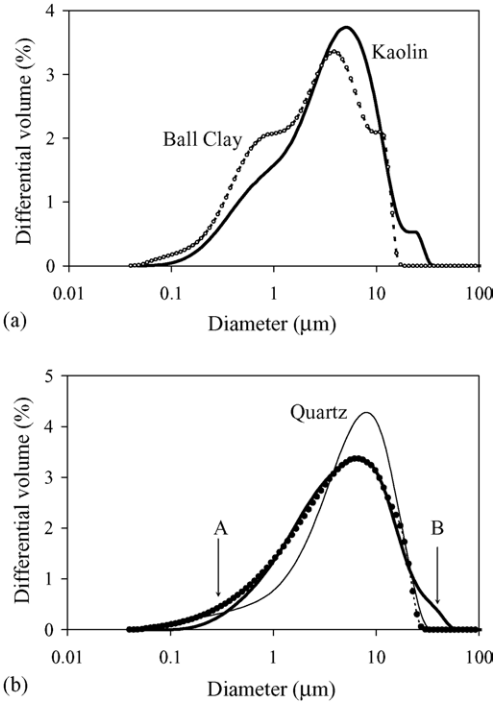

Fig. 1. Particle size distribution of the raw materials used in the batches of the model porcelain formulations: (a) plastic raw materials; (b) hard materials.

The following techniques were employed: particle size distribution, using light-scattering equipment (Coulter LS 230, UK, Fraunhofer optical model). Dilatometry of green porcelain bodies (Bahr Thermo Analyse DIL 801 L, Germany, heating rate 10°/min). X-ray diffraction analysis (XRD, Rigaku Geigerflex D/Mac, C Series, Cu Ka radiation, Japan). Microstructure observation (SEM, Hitachi S-4100, Japan, 25 kV acceleration voltage) at polished and etched surfaces (immersion in 2 vol.% HF for 4 min). Measurement of whiteness (portable colorimeter Minolta CM-508-d 1998, Japan, Hunter method). Archimedes method (immersion in ethylenoglycol) to determine the apparent density. Flexural strength (three-point bending) was measured with parallelepiped bars (3 mm × 4 mm × 40 mm) (Shimadzu Autograph AG 25 TA, 0.5 mm/min displacement; the presenting results are the average of 16 bars). Water absorption was measured according to the ISO-standard 10545-3, 1995, i.e. weight gain of dried bulk samples after immersion into boiling water for 2 h, cooling for 3 h and sweeping of their surface with a wet towel. The linear shrinkage during sintering was also calculated from the dimensions of the green and the sintered samples.

3. Results

3.1. Densification of the model porcelain bodies

Fig. 2 summarizes the results of density, shrinkage and water absorption of the model porcelains measured after firing at different temperatures. Obviously, the amount of added Li_2CO_3 into the batch of the standard triaxial porcelain formulation considerably affected the sintering behaviour and the properties of the fired porcelains. The samples of L1, L2 and L3 exhibited similar general features and were successfully sintered at much lower temperatures than L0.

Further increasing the Li_2CO_3 content in the batch (i.e. L4–L7) caused significant reduction of shrinkage and density at the temperature range of maximum densification, which was more pronounced in the case of L6 and L7. The relatively high values of water absorption of L6 and L7 seemingly indicate that these compositions had undergone incomplete sintering. The abnormal change of water absorption values of L7 between 1300 and 1350 °C is due to over firing effect followed by fast vitrification at 1350 °C, confirmed by the obvious rounding of the sharp edges of the cylindrical pellets. This effect indicates a short firing range of this formulation.

Increasing Li-content causes significant changes in the crystalline phases formed (1300 °C, Fig. 3). Together with

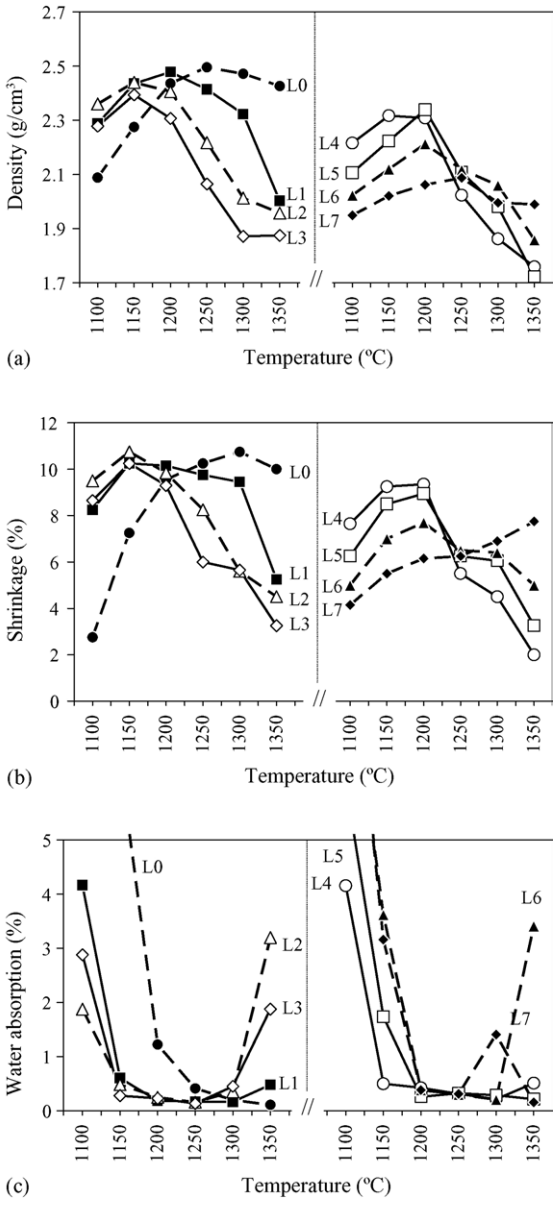

Fig. 2. The influence of firing temperature on: (a) density, (b) shrinkage and (c) water absorption of the model porcelains (the standard deviation of the presented points was less than 5%).

quartz, the peaks of mullite are intense in L1 and L2 but significantly degenerated at higher contents of Li_2O (L3, L4). The crystalline phase formation of L7 was completely different, comprising predominantly a Li-associated phase ($LiAlSi_3O_8$) and alumina, and traces of mullite. The formation of the former two phases has evidently started from L5 and L6.

Another important feature of the L6 and L7 samples was their pink colour appearing after sintering at temperatures ≥1150 °C. The strongest pink colouring effect was observed in the L7 fired at 1300 °C, which then turned to white colour after firing at 1350 °C, likely due to vitrification.

Consequently, among the investigated model formulations, L1 and L2 porcelains exhibited complete densification

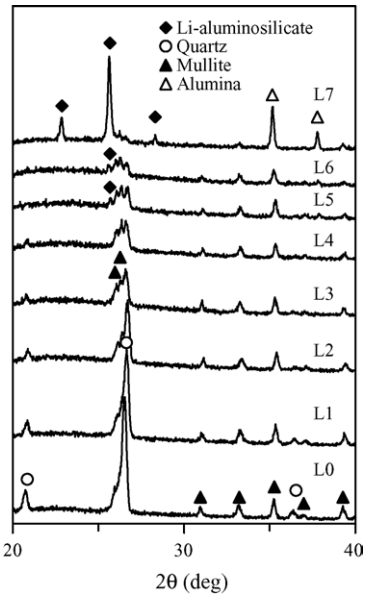

Fig. 3. XRD spectra of the model porcelains fired at 1300 °C (JCPDS cards: quartz 46-1045; mullite: 15-0776; lithium aluminium silicate ($LiAlSi_3O_8$): 35-0794; alumina: 75-1863).

in the temperature range between 1200 and 1250 °C, which is considerably lower than the maturation temperature of the standard triaxial porcelain (~1350 °C). Therefore, the design of low temperature porcelains containing natural bearing pegmatite was focused on formulations whose Li_2O-content approached porcelains L1 and L2 (0.44 and 0.88 wt.% Li_2O, respectively).

3.2. Synthesis and properties of low temperature porcelain bodies containing natural Li-bearing pegmatites

In the light of the previous conclusion, the compositions of the porcelain bodies with Li-bearing pegmatites, A and B (Table 3), were designed as follows: (a) The ratios among clay minerals, fluxes and quartz were almost equal to that of the standard hard porcelain L0; (b) The amount of flint (i.e. quartz, Table 3) was calculated taking into account the quantity of free quartz introduced in the batch by the lithium-bearing pegmatites (Table 4); (c) The incorporated amount of Li_2O introduced via the Li-bearing pegmatites was adjusted at 0.5 wt.% (composition B) and 0.9 wt.% (composi-

Table 4
Calculated mineralogical composition of Li-bearing pegmatites (wt.%) (see also note of Table 1)[20,21]

Minerals	Li-bearing pegmatite A	Li-bearing pegmatite B
Albite	~10	~22
Microcline	~20	~15
Muscovite	~12	~9
Spodumene	~30	–
Petalite	–	~29
Free quartz	~29	~22

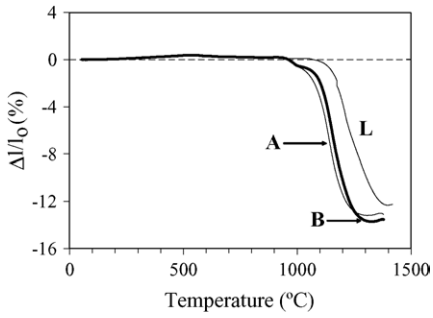

Fig. 4. Shrinkage behaviour of porcelain bodies made of the formulations A, B and L.

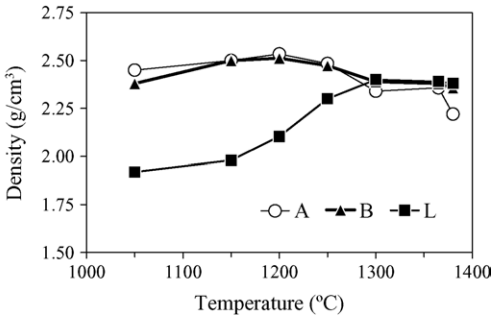

Fig. 5. The influence of firing temperature on density of the fired porcelains A, B and L (the standard deviation of the presented points was less than 5%).

tion A), to resemble the Li_2O-content of L1 and L2, respectively (Table 2).

The dilatometry curves (Fig. 4) indicate earlier shrinkage of porcelain bodies A and B (∼970 °C) than the conventional composition L (∼1080 °C). Densification occurs slightly faster in composition A and achieves maximum shrinkage at ∼1270 °C. With regards to shrinkage, both compositions exhibited better sintering ability than L (whose maximum shrinkage was recorded at 1390 °C). The stability of shrinkage values of composition A between 1270 and 1380 °C indicates expanded maturation range and high deformation resistance during firing for A. The composition B exhibited similar behaviour reaching maximum shrinkage at ∼1290 °C but the maturing range is seemingly 20–25 °C shorter than that of A.

The influence of firing temperature on the density of porcelain bodies is plotted in Fig. 5. Densification of the Li-containing porcelains A and B occurred early, reaching relatively high density already at 1050 °C (2.45 g/cm^3 for A and 2.38 g/cm^3 for B), and maximum density of 2.48–2.53 g/cm^3 between 1150 and 1250 °C, while overfiring effect was observed at ≥1300 °C (density dropped to ∼2.35 g/cm^3). The bodies of the reference porcelain L were still fragile and poorly dense at the lower tested temperatures, while the temperature range of maximum density was significantly higher (1300–1350 °C).

The values of the properties of porcelain bodies of A and B fired at 1150, 1250 and 1365 °C (the last one corresponds to the industrial kiln firing), presented in Table 5, agree fairly well to the previous conclusions (Fig. 5). At this point it is worthy nothing that the results of firing tests carried out in industrial tunnel kiln at 1365 and 1380 °C showed that the porcelain bodies of the Li-containing compositions A and B successfully maintained their good properties at temperatures much higher than those anticipated for proper sintering by Fig. 5 and Table 5 (i.e. 1150–1250 °C), while the appearance of the samples did not indicate evidence of overfiring effect (i.e. deformation, formation of bubbles, etc.).

The maturation of porcelain L occurred between 1300 and 1400 °C. At 1365 °C density was 2.45 g/cm^3, shrinkage 13.6%, water absorption 0.11%, bending strength 80.50 (±5.48) MPa, and whiteness 79.85%.

3.3. Phase evolution and microstructure of Li-bearing pegmatite containing porcelains

Fig. 6 plots the XRD spectra of the porcelains A, B and L fired at elevated temperatures (1150–1365 °C). Mullite and α-quartz were detected at all temperatures. There is no evidence of formation of Li-associated phases. It is obvious that the highest crystallinity (especially with regards to mullite) is achieved at 1250 °C for A and B and at 1365 °C for L, whereas the crystallinity of A and B significantly decreases.

SEM observations indicated no perceptible difference between the microstructure of A and B. Firing at 1150 °C resulted in a well sintered structure comprising the crystalline phases and pores dispersed in a glassy matrix (Fig. 7a). At higher magnification (Fig. 7b), we can distinguish the coarse

Table 5
Properties of the porcelain bodies A and B fired in laboratory electric furnace (1150 and 1250 °C) and industrial tunnel kiln furnace (1365 °C)

Temperature (°C)	Density (g/cm^3)	Shrinkage (%)	Water absorption (%)	Bending strength (MPa)	Whiteness (%)
A					
1150	2.45	14.1	0.14	–	–
1250	2.53	15.6	0.12	79.72 ± 10.14	–
1365	2.36	15.3	0.14	78.34 ± 7.76	77.46
B					
1150	2.38	16.4	0.14	–	–
1250	2.51	16.4	0.07	92.81 ± 5.05	–
1365	2.38	15.4	0.16	82.57 ± 8.68	78.63

Bending strength was measured only at the denser materials, and whiteness only at the porcelains fired in the tunnel kiln since high whiteness was obtained due to the reduction atmosphere.

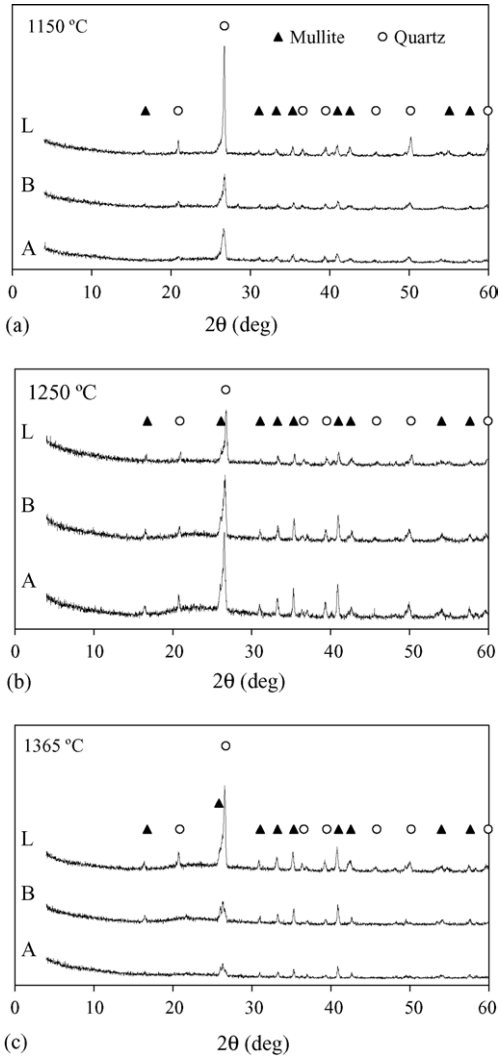

Fig. 6. XRD spectra of the porcelains A, B and L fired at: (a) 1150 °C, (b) 1250 °C and (c) 1365 °C (JCPDS cards: quartz 46-1045; mullite: 15-0776).

quartz grains and the needle-like secondary mullite. Feldspar relicts with needle-like secondary mullite crystals surrounded by clay relicts region with primary mullite scaly crystals were also clearly observed (Fig. 7c).

Firing at 1250 °C caused slight increase of pore size (Fig. 8a), probably resulted from gas evolution due to reduced viscosity of the glassy phase.[19,22] The latter phenomenon also causes development and growth of secondary mullite needles at the expense of small primary mullite crystals, which are dissolved in the melt and further recrystallized in the form of needles (Fig. 8b).

Overfiring, seemingly occurred at 1365 °C, resulted in relatively large pores (>10 μm)[23] and strong dissolution of quartz grains (Fig. 9a). Elongated mullite crystals (∼4 μm) were embedded in a glassy matrix (Fig. 9b).

The porcelain bodies made of the L composition fired at 1365 °C featured the typical microstructure of triaxial porcelains,[1,19] which comprises quartz grains surrounded with the characteristic glass rim, mullite crystals (primary and

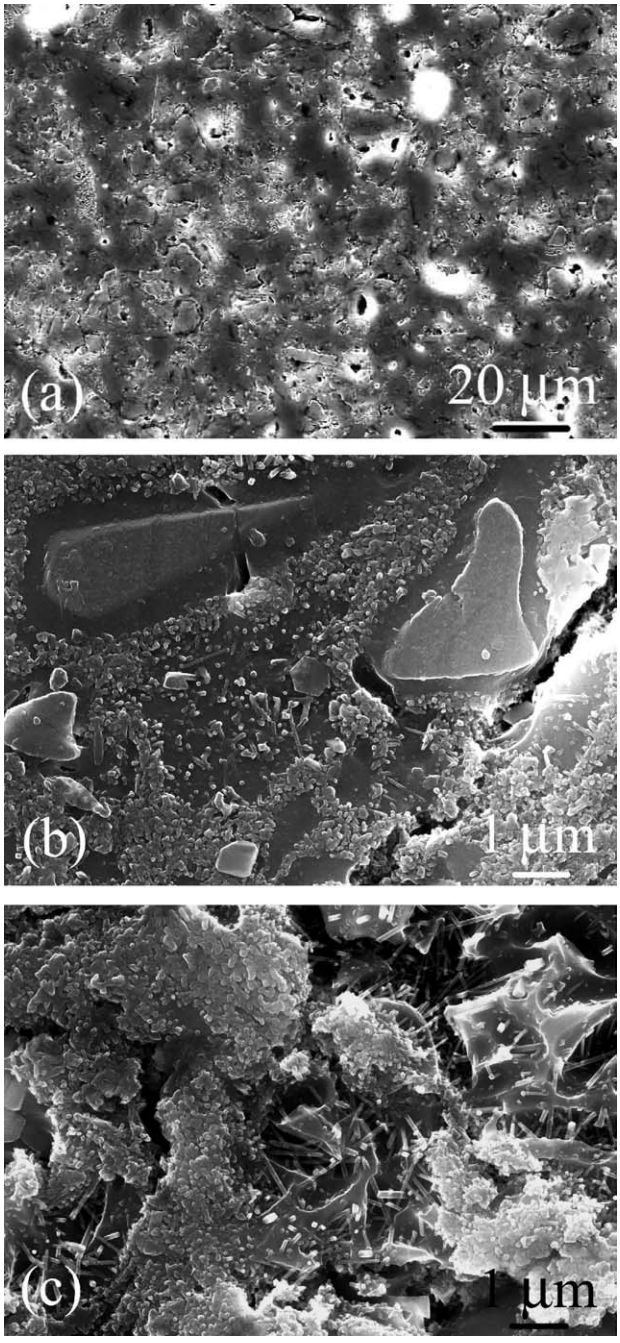

Fig. 7. Microstructure of the model porcelain B fired at 1150 °C. Similar characteristics were observed in the model porcelain A (see the text for a more detailed description).

secondary) and pores distributed in aluminosilicate glassy phase.

4. Discussion

Under an industrial perspective, the most important finding of this study is that the Li-bearing compositions A and B, whose design was based on the experimental findings with

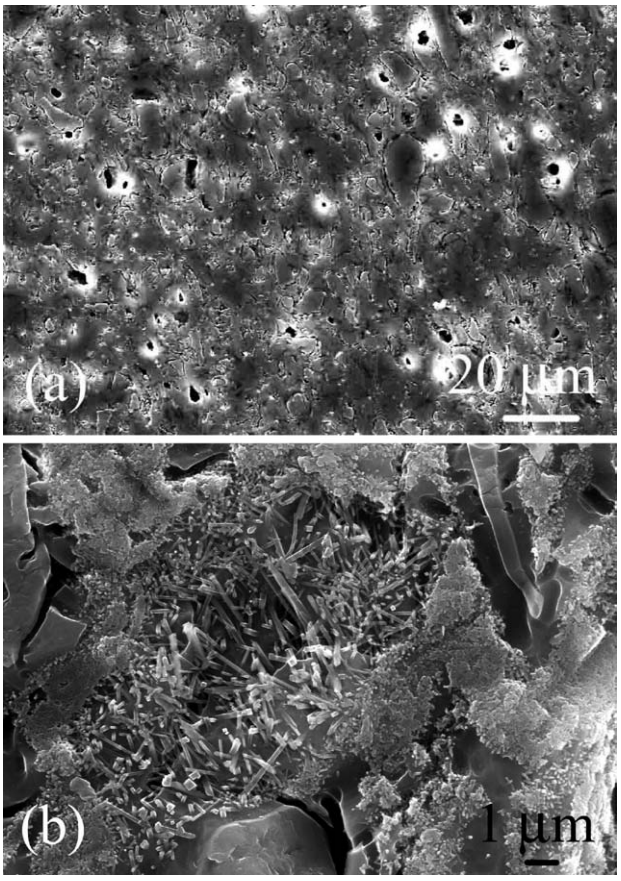

Fig. 8. Microstructure of the model porcelain B fired at 1250 °C. Similar characteristics were observed in the model porcelain A (see the text for a more detailed description).

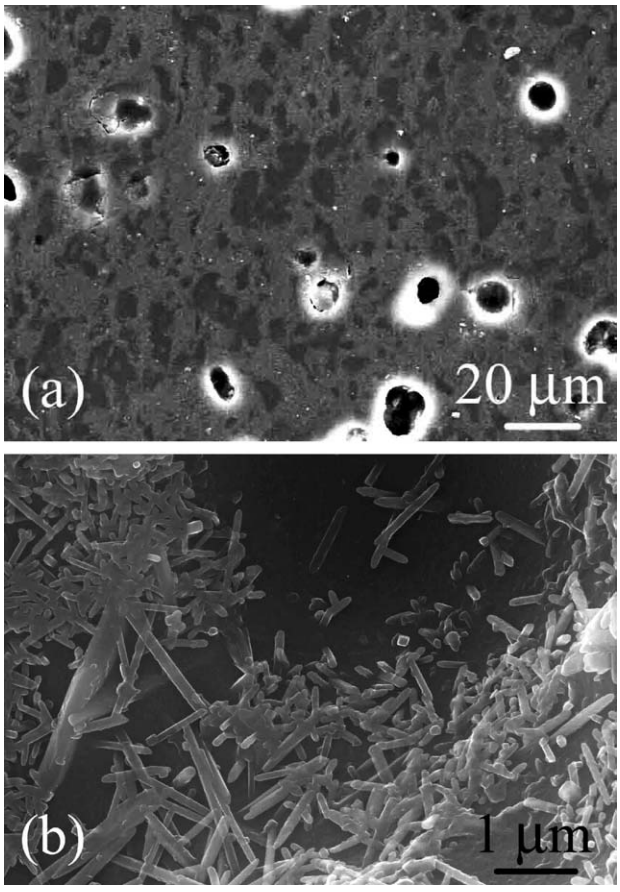

Fig. 9. Microstructure of the model porcelain B fired at 1365 °C. Similar characteristics were observed in the model porcelain A (see the text for a more detailed description).

the model formulations, reached maximum shrinkage at temperatures 100–120 °C lower than the conventional L formulation (Fig. 4). Taking into account the influence of heating rate on shrinkage measurements (10°/min in dilatometry, 4°/min in the laboratory furnaces, and 2.5°/min in the industrial kiln), the actual curves of shrinkage have been shifted towards higher temperatures in Fig. 4. Accordingly, the maturation of A and B compositions (i.e. maximum density and shrinkage values, Table 5) actually occurs between 1150 and 1250 °C. Moreover, despite the significant reduction of density, firing at 1365 °C caused no noticeable degradation of the quality and the properties of the porcelain bodies A and B. The maturation of the standard triaxial porcelain L ranged between 1300 and 1400 °C. The temperature range of gloss firing of standard triaxial porcelain items in industrial conditions usually takes place at 1350–1400 °C.[1,2]

The firing of triaxial porcelain bodies occurs according to the following general stages:[1,2,24–29] (a) at ∼550 °C kaolinite is transformed into metakaolinite; (b) at 573 °C α-quartz is inversed to β-quartz; (c) at 950–1000 °C metakaolinite is transformed to a spinel-type structure and amorphous free silica; (d) at 985 °C the eutectic orthoclase-silica melts, resulting in the first liquid phase; (e) at ∼1100 °C primary mullite forms in the clay relicts, potassium feldspar melts, and alkalis are diffused out of feldspar; and (f) The final stage of firing comprises nucleation and growth of secondary mullite and dissolution of quartz.

Similarly to L composition, mullite and quartz were exclusively detected in the A and B compositions (Fig. 6). Therefore, the lithium should be dissolved in the glassy phase. Accordingly, the firing of the porcelains A and B would be described under the following concept. In properly mixed unfired porcelain batch, quartz, feldspar, spodumene (or petalite) and muscovite are generally surrounded by clay minerals. After the transformation of kaolinite and quartz, muscovite looses a major part of the chemically bonded water (>850 °C) and α-spodumene (or α-petalite) undergo structural changes. In naturally occurring rocks, low temperature α-spodumene (or α-petalite) is inversed to high temperature β-spodumene at 900–1000 °C,[20,30,31] but Fig. 6 does not evidence such reaction in either A or B porcelains. Evidently, lithium, which has small ionic radius, was diffused in the particles of metakaolinite, which exhibits high surface area and pore–volume distribution after metakaolinisation.[11] The presence of lithium probably causes reduction of the eutectic point at the feldspar/metakaolinite boundary, promoting formation of glass phase at these interfaces. Both phenomena

(i.e. lithium diffusion and early melting) in conjunction with the diffusion of potassium and sodium ions from feldspar and muscovite to clay relicts should favour densification of clay relicts and crystallization of primary mullite.

Earlier studies have demonstrated that primary mullite serves as nucleation seed of secondary mullite, whose crystals originate from the outer surface of clay and grow into the less viscous feldspar relicts.[18,32] In standard triaxial porcelains, secondary mullite crystals form at 1200 °C,[18] but in the Li-containing compositions, studied in the present work, acicular secondary mullite crystals were observed after firing at 1150 °C (Fig. 7b). The diffusion of alkalis from muscovite and spodumene (or petalite) may also cause favourable changes of the compositions with respect to secondary mullite formation.

Primary scaly mullite was dissolved and recrystallized in form of secondary mullite needles between 1150 and 1250 °C, resulting in increasing crystallinity (Figs. 6, 7c and 8b). Earlier studies with porcelains, whose batches had high contents of feldspar or nepheline syenite, have demonstrated that the crucial point of successful firing and high quality of the produced porcelains is the optimum amount of liquid phase resulted from the dissolution of quartz.[29] Therefore, the same amount of the optimum liquid in the porcelain body is evidently formed at lower temperatures in the case of A and B porcelains and at higher temperatures in the standard porcelain L. Although, firing of A and B at 1250 °C evidently caused formation of higher amount of liquid (Fig. 5), the remarkable resistance to pyroplastic deformation and the maintenance of the high mechanical strength after firing at extreme conditions (>1350 °C) can be due to mullite crystals, which have effectively increased in size in the viscous glassy phase (Fig. 9b).[29]

Consequently, this work showed that incorporation of small quantity of Li_2O in the raw materials opens great potential in porcelain industry. Indeed, great differences were detected between the non-doped formulations (L and L0) and the Li-doped ones L1, L2, A and B. With respect to tableware porcelains, the experimental results with the model compositions indicated that desirable properties can be attained if the Li_2O-content does not exceed ~1.5 wt.%. Indeed, the L3 composition maintained good properties (like L1 and L2) but the maturation temperature range was significantly shorter (Fig. 2a, 2b). Further increase beyond this limit (L4–L7) resulted in products with poorer properties and significantly shorter maturation temperature range.

The influence of Li_2O-content on the properties can be interpreted as follows. Fig. 3 shows that the maximum intensity of the mullite peaks was observed in L1 and L2. These compositions (together with A and B) exhibited the best properties. The same phases were formed in L3 and L4 but their X-ray intensities were significantly lower. The intensity of the peaks of mullite and quartz further decreased in L5 and L6 but formation of spodumene s.s. (lithium orthoclase, $LiAlSi_3O_8$) and alumina occurred, which were the dominant phases in L7. These results indicate that increasing of Li_2O-content over 1.5 wt.% seemingly opposes (and probably inhibits) the formation of mullite. In the case of formation of spodumene s.s., density probably decreases because spodumene has much lower density than mullite ($d_{\beta\text{-spodume}} = 2.35\ g/cm^3$, $d_{mulite} = 3.00\ g/cm^3$). The pink colouring in the case of the high Li_2O-content formulations is another serious problem in industrial porcelain production. Development of pink spots has been reported in the case of materials made of mullite–spodumene and spodumene with Fe_2O_3.[11]

5. Conclusions

The experimental results with the model formulations showed that desirable properties for tableware porcelains can be attained if the Li_2O-content does not exceed ~1.5 wt.%. This essential conclusion was the key to design the new porcelain formulations using Li-bearing natural rocks. Under an industrial perspective, the most important finding is that these compositions matured at temperatures 100–120 °C lower than the triaxial porcelain formulation and exhibited remarkable resistance at over-firing conditions.

Consequently, incorporation of small quantity of Li_2O in the raw materials seemingly features great potential in porcelain industry. Analysis of the experimental results indicates that Li_2O plays important role in the mechanism that occurs at the different stages of firing, as indicted by the influence of increasing Li_2O-content on densification, the evolution of crystalline phases and microstructure at different temperatures.

Acknowledgement

This study was supported by CICECO and the Portuguese FCT.

References

1. Carty, W. M. and Senapati, U., Porcelain-raw materials, processing, phase evolution, and mechanical behaviour. *J. Am. Ceram. Soc.*, 1998, **81**, 3–20.
2. Avgustinik, A. I., *Ceramics* (*2nd ed.*). Stroiizdat, Leningrad, 1975 [in Russian].
3. Noirot, M. D., Formulating porcelain bodies with borax auxiliary flux. *Ceram. Eng. Sci. Proc.*, 2002, **23**, 57.
4. Tulyaganov, D. U., Lopez-Cuevas, J., Mendell-Nonell, J. and Ismatov, A., Whiteware bodies with low deformation characteristics. *Am. Ceram. Soc. Bull.*, 2001, **80**, 65–68.
5. Baumgart, W., Dunham, A. C. and Amstutz, G. C., Lithium aluminosilicates. In *Process Mineralogy of Ceramic Materials*, ed. W. Baumgart. Ferdinand Enke Publishers, Stuttgart, Germany, 1984, pp. 9–10.
6. Cowan, C. A., Bole, G. A. and Stone, R. L., Spodumene as a flux component in sanitaryware bodies. *J. Am. Ceram. Soc.*, 1950, **33**, 193–197.
7. Low, I., Mathews, E., Garrod, T., Zhou, D., Philips, D. N. and Pillai, X. M., Processing of spodumene-modified mullite ceramics. *J. Mater. Sci.*, 1997, **32**, 3807–3812.

8. Smoke, E. J., Ceramic compositions having negative thermal expansion. *J. Am. Ceram. Soc.*, 1951, **34**, 87–90.
9. Fishwick, J. H., Van der Beck, R. R. and Talley, R. W., Low thermal expansion coefficients in the systems spodumene–kaolin and petalite–kaolin. *Am. Ceram. Soc. Bull.*, 1964, **43**, 832–835.
10. Abdel-Fattah, W. I. and Abdellah, R., Lithia porcelains as promising breeder candidates—I. Preparation and characterization of β-eucriptite and β-spodumene porcelain. *Ceram. Int.*, 1997, **23**, 463–469.
11. Yamuna, A. and Devanarayanan, S., Mullite–β-spodumene composites from aluminosilicates. *J. Am. Ceram. Soc.*, 2001, **84**, 1703–1709.
12. Lundin, S. T., In *Studies on Triaxial Whiteware bodies*. Almqvist and Wiksell, Stockholm, Sweden, 1959.
13. Holmstrom, N. G., Fast-firing of triaxial porcelain. *Am. Ceram. Bull.*, 1981, **60**, 470–473.
14. Funk, J. E., Designing the optimum firing curve for porcelains. *Am. Ceram. Soc. Bull.*, 1982, **62**, 632–635.
15. Rado, P., The strange case of hard porcelain. *Trans. Br. Ceram. Soc.*, 1971, **71**, 131–139.
16. Schüller, K. H., Reactions between mullite and glassy phase in porcelains. *Trans. Br. Ceram. Soc.*, 1964, **63**, 103–117.
17. Schüller, K. H., In *Process Mineralogy of Ceramic Materials*, ed. W. Baumgart. Ferdinand Enke, Stuttgart, Germany, 1984.
18. Iqbal, Y. and Lee, W. E., Fired porcelain microstructures revisited. *J. Am. Ceram. Soc.*, 1999, **82**, 3584–3590.
19. Iqbal, Y. and Lee, W. E., Microstructural evolution in triaxial porcelain. *J. Am. Ceram. Soc.*, 2000, **83**, 3121–3127.
20. Charoy, B., Noronha, F. and Lima, A., Spodumene–petalite–eucryptite: mutual relationships and pattern of alteration in Li-rich aplite–pegmatite dykes from northern Portugal. *Can. Minerol.*, 2001, **39**, 729–746.
21. Amarante, M. M., de Sousa, A. B. and Leite, M., Technical note processing a spodumene ore to obtain lithium concentrates for addition to glass and ceramic bodies. *Miner. Eng.*, 1999, **12**, 433–436.
22. Norris, A. W., Taylor, D. and Thorpe, I., Range curves: an experimental method for the study of vitreous pottery bodies. *Trans. Br. Ceram. Soc.*, 1979, **78**, 102–108.
23. Chu, G. P. K., Microstructure of complex ceramics. In *Ceramic Microstructures, Their Analysis, Significance, and Production*, ed. R. M. Fulrath and J. A. Pask. Wiley, New York, 1968, Chapter 38, pp. 843–844.
24. Brindley, G. W. and Nakahira, M., The kaolinite–mullite reactions series. III The high temperature phases. *J. Am. Ceram. Soc.*, 1959, **42**, 319–323.
25. Schneider, H., Okada, K. and Pask, J., In *Mullite and Mullite Ceramics*. Willey, New York, 1994, p. 106.
26. Okada, K., Otsuka, N. and Ossaka, J., Characterization of spinel phase formed in the kaolinite–mullite thermal sequence. *J. Am. Ceram. Soc.*, 1986, **69**, C-251–C-253.
27. Maitu, S., Mukhopadhyay, T. K. and Sarkar, B. K., Silimanite–sand–feldspar porcelains: I. Vitrification behavior and mechanical properties. *Interceramics*, 1996, **45**, 305–312.
28. Maitu, S. and Sarkar, B. K., Development of high-strength whiteware bodies. *J. Eur. Ceram. Soc.*, 1996, **16**, 1083–1088.
29. Carty, W. M., Observation on the glaze phase composition on porcelains. *Ceram. Eng. Sci. Proc.*, 2002, **23**, 79–94.
30. Kukolev, G. V., In *Silicon Chemistry and Physical Chemistry of Silicates*. Vysshaya Shkola, Moscow, 1966 [in Russian].
31. Pannhorst, W., In *Low Thermal Expansion Glass Ceramics*, ed. H. Bach. Springer-Verlag, Berlin, 1995, pp. 1–12.
32. Lundin, S. T., Microstructure of porcelain. In *Microstructure of Ceramic Materials. Proceedings of the American Ceramic Symposium, National Bureau of Standards Miscellaneous Publications No. 257*. National Bureau of Standards, Gaithersburg, MD, 1964, pp. 93–106.